Longitudinal oscillations and flights of the string pendulum driven by a periodic force

A. Arinstein
Department of Mechanical Engineering, Technion–Israel Institute of Technology, Haifa 32000, Israel
(Received 7 January 2009; revised manuscript received 1 April 2009; published 22 May 2009)

The longitudinal oscillations of a string pendulum are discussed. The regime in which the oscillating bob executes free flight under gravity is studied. This regime arises if, during the motion in the upward direction, bob reaches a height at which no elastic force acts on bob, and its further motion occurs only under gravity. Thus, the string pendulum executes a motion of two types: the harmonic oscillations under the action of elastic force and free flights under gravity. In doing so, the height of flights can considerably exceed the amplitude of the forced oscillations, i.e., a noticeable amplitude amplification in the longitudinal oscillations of a string pendulum takes place. A mechanism of a resonance phenomenon related to the excitation of free oscillations is described. These free oscillations arising after each bob flight are the channel for energy pumping into the system in question. It turns out that the frequency of the above resonance is equal to the fundamental frequency of the string, and the resonance amplitude of the flights is proportional to the square of amplitude of regular forced oscillations.

DOI: 10.1103/PhysRevE.79.056609 PACS number(s): 45.30.+s, 05.45.−a

I. INTRODUCTION

The pendulum is the simplest toy system, which allows one to examine both linear harmonic oscillations and nonlinear ones. Since a pendulum model has many applications in different fields of science and techniques, tremendous effort has gone into the study of the pendulum. It is worth mentioning the recent book *The Pendulum*, devoted to scientific, historical, philosophical, and educational perspectives for the pendulum modeling [1], and the *International Pendulum Conference* [2] (containing more than 500 references). First of all, the analysis of various pendulum models is a good way for a study of regular and chaotic motion [3–9]. Some nonlinear pendulum models can serve as a basis for equipment development. For example, the water-based friction modifier for railway applications was modeled by means of the nonlinear pendulum [10]; a pendulum analogy was used for the development of methods for slosh parameter estimation [11]; a folded pendulum isolator has been suggested for evaluating accelerometer performance [12], etc. The majority of these and many other references discuss the nonlinear features of the spring pendulum, while only three of them examine string pendulum behavior [7–9]. Such disproportion is related to the fact that the behavior of both spring and string pendulums is identical if the amplitude of oscillations is not too large. A difference between the spring and string pendulums is that the latter possesses the additional degree of freedom related to the flexibility of a string. The flexibility of a string results in the fact that a string pendulum which executes planar oscillations demonstrates nonlinear behavior, even if the amplitude of these oscillations is not very large [8]. The increase in the oscillation amplitude leads to a new phenomenon; the oscillating mass, upon reaching a certain height, leaves the circular trajectory corresponding to planar oscillations and executes a jump under gravity (along a parabolic path) until the string is again stretched [9].

Just jumps (or flights) are of interest to us in the study of the longitudinal oscillations of a string pendulum. Indeed, the longitudinal oscillations of a forced string pendulum can occur according to the following scenario. If the amplitude of the external excitation is large enough and/or its frequency is close enough to the resonant one, then the amplitude of the forced oscillations can exceed the string elongation due to gravity acting on bob. In such a case, when the motion is in the upward direction, bob can reach a height at which no elastic force affects bob, its further motion occurring only under gravity, i.e., bob executes free flights. In other words, the string pendulum executes motion of two types: the harmonic oscillations under the action of the elastic force and free flights under gravity. In doing so, the height of flights can considerably exceed the amplitude of the forced oscillations (by a factor of 5–10 or more).

Such a phenomenon allows one to increase the visible displacement of an oscillating bob. This fact can find useful applications in nanotechnology, allowing one to exploit instrumentation having limited accuracy. Moreover, the actual motivation for the following analysis is the development of a nondestructive method for the mechanical testing of individual nanofibers [13]. Briefly, the idea of this method is the following: using a nanofiber as a string with the suspended bob (see photograph in Fig. 1), one can find the resonant frequency of such a string pendulum, and thereby determine the Young's modulus of the nanofiber. Bob jumps, alone, allowing one to obtain experimental data, operating only with an optical microscope. (Note that the allowable amplitudes of regular oscillations in the elastic mode are below the resolution limit of any optical microscope.)

II. MATHEMATICAL DESCRIPTION OF THE SYSTEM

We examine a pendulum consisting of a string having a free length, l_0, and stiffness constant, κ, and of a suspended bob of mass m. In the equilibrium position, where the elastic stress of a string is balanced by gravity acting on bob, the string elongation, Δl, is [see Fig. 1(a)]

$$\Delta l = mg/\kappa. \tag{1}$$

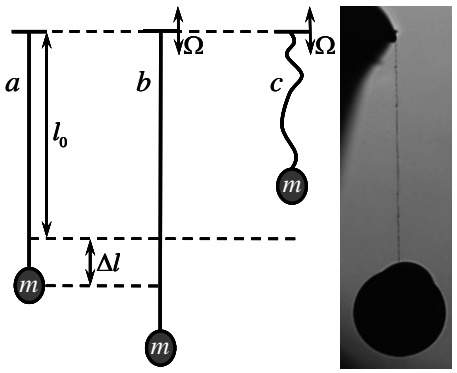

FIG. 1. The string pendulum: (a) the equilibrium state of the pendulum with the string elongation Δl; (b) the downward displacement of bob, at which string remains stretched; (c) the bob flight at the upper displacement when the string becomes unstrained. The photograph demonstrates a string pendulum (consisting of a nanofiber with suspended bob) being used for mechanical testing of individual nanofibers.

Let us choose the origin to be located at the suspension point with an upward x axis. In our coordinate system, the equilibrium position of bob is defined by $x_0=-(l_0+\Delta l)$. A displacement of the oscillating bob is Δx; thus, its coordinate is $x=x_0+\Delta x=\Delta x-(l_0+\Delta l)$. If the suspension point executes oscillations, $A\sin(\Omega t)$, the resultant force acting on bob is $F=\kappa[A\sin(\Omega t)-\Delta x]$, and the motion equation is

$$m\frac{d^2\Delta x}{dt^2}=\kappa[A\sin(\Omega t)-\Delta x]-\mu\frac{d\Delta x}{dt}, \tag{2}$$

where μ is the effective friction coefficient. Equation (2) is true if bob is moving in the downward direction [see Fig. 1(b)] or if its upper displacement Δx is not too large, and the string remains stretched, namely, $\Delta x<A\sin(\Omega t)+\Delta l=A\sin(\Omega t)+mg/\kappa$.

In the opposite case of large upward displacements, when $\Delta x>A\sin(\Omega t)+mg/\kappa$, the string becomes unstrained, and bob moves only under gravity [see Fig. 1(c)], and the motion equation in this case is

$$m\frac{d^2\Delta x}{dt^2}=-mg. \tag{3}$$

Using the dimensionless displacement $u=\Delta x/\Delta l=\Delta x\omega_0^2/g$, and the dimensionless time $\tau=\omega_0 t$ ($\omega_0^2=\kappa/m$ is the natural frequency of the oscillating bob), Eqs. (2) and (3) can be transformed into the following form:

$$\frac{d^2u}{d\tau^2}+2\gamma\frac{du}{d\tau}+u=a\sin(\Omega_0\tau),\quad u<1+a\sin(\Omega_0\tau), \tag{4}$$

$$\frac{d^2u}{d\tau^2}=-1,\quad u>1+a\sin(\Omega_0\tau), \tag{5}$$

where $\gamma=\mu/2m\omega_0$ is the damping factor, $\Omega_0=\Omega/\omega_0$, and $a=A/\Delta l=A\omega_0^2/g$.

Equation (4) describes the longitudinal oscillations of a suspended bob, whereas Eq. (5) describes its free flights when the string becomes unstrained. Note that the stages of oscillation (both free and forced) and of flight alternate with one another, in doing so, the initial conditions for each stage are determined by the motion in the previous one.

III. NUMERICAL SIMULATION

In order to illustrate the features of the system in question one can solve the equation systems (4) and (5) numerically. The necessary numerical calculations were performed using the MATHCAD program with the help of the built-in function *ordinary differential equation solve blocks* (*Odesolve*). Typical results of such calculations are pictured in Fig. 2.

One can see that the displacement of the oscillating bob in the upward direction is much larger than in the downward one. These large displacements in the upward direction correspond to the flights of bob since the curve of the bob trajectory (thick solid line) is situated higher than the line corresponding to the stretched-unstrained boundary, $1+a\sin(\Omega_0\tau)$ (thin solid line). In doing so, the flight time amounts to several periods of external force, whereas the time of each oscillatory stage corresponds to only half of this period.

The Poincare's cross sections of the solutions of Eqs. (4) and (5) are presented in Fig. 3. Both plots in this figure demonstrate that the chaotic behavior of the system in question is observed, and in doing so, attractors arise. Note that the attractors are observed in the case of both resonant and nonresonant frequencies of the external force.

In order to justify the system stochastisation, two independent numerical solutions were compared. The first solution was obtained for the following initial conditions: $u_1(0)=0$ and $\dot{u}_1(0)=a\Omega_0$. The initial conditions for the second

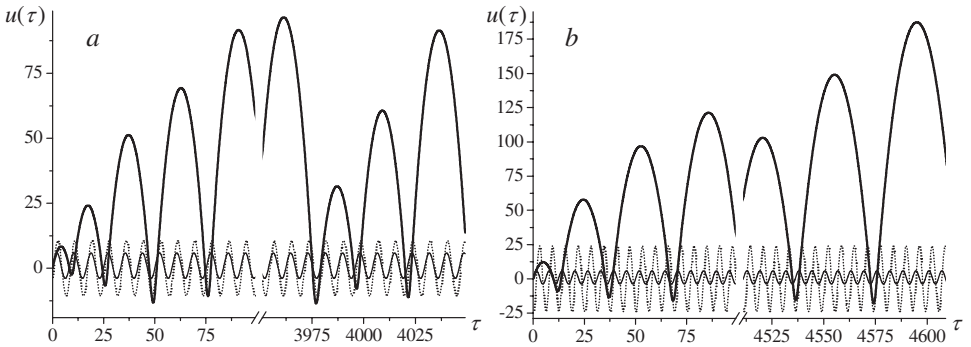

FIG. 2. The numerical solution of Eqs. (4) and (5) (the thick solid line) for $a=5$ and $\gamma=0.1$. (a) $\Omega_0=0.75$; and (b) $\Omega_0=1$ (resonance frequency). The thin solid line corresponds to the stretched-unstrained boundary $1+a\sin(\Omega_0\tau)$, and the dotted line corresponds to the forced oscillations of the equivalent spring pendulum.

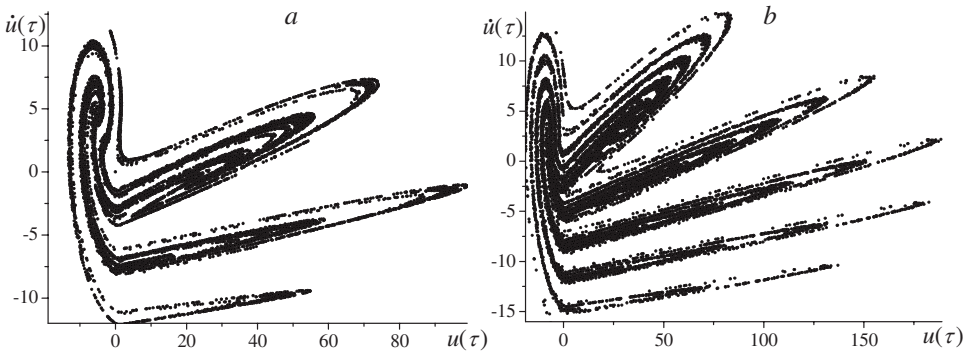

FIG. 3. The Poincare's cross section of solutions of Eqs. (4) and (5) pictured on Fig. 2 for $a=5$ and $\gamma=0.1$. (a) $\Omega_0=0.75$; and (b) $\Omega_0=1$ (resonance frequency).

solution were defined as $u_2(0)=u_1(\delta\tau)$ and $\dot{u}_2(0)=\dot{u}_1(\delta\tau)$. Thereafter the time point, $\delta\tau$, was assumed as the new starting point for the first solution, so that the solutions $u_1(\tau+\delta\tau)$ and $u_2(\tau)$ were being compared. The calculation results obtained for $a=5$, $\gamma=0.1$, $\Omega_0=1$, and $\delta\tau=0.01$ are pictured in Fig. 4(a). One can see that in spite of the fact that at the initial stage these two solutions coincide, after some time they deviate from one another, and finally become independent (uncorrelated). This last fact can be verified with the help of the correlation function,

$$G(\tau)=\frac{\int_0^\tau [u_1(t+\delta\tau)-\bar{u}_1][u_2(t)-\bar{u}_2]dt}{\sqrt{\int_0^\tau [u_1(t+\delta\tau)-\bar{u}_2]^2 dt \int_0^\tau [u_2(t)-\bar{u}_2]^2 dt}}, \quad (6)$$

where $\bar{u}_{1,2}=\lim_{t\to\infty}\frac{1}{t}\int_0^t u_{1,2}(t)dt$. The calculations result in an exponential decay of the correlation function (6) [see Fig. 4(b)]. The asymptotic low-correlation degree can be attributed to attractors arising in the Poincare's cross sections (see Fig. 3). Note that though the results shown in Fig. 4 are obtained for the resonant frequency of the external force ($\Omega_0=1$), such behavior is typical also for other frequencies of the external force, and the difference consists of the stochastisation rate and of the asymptotic value of the correlation function. The obtained numerical results are a good argument in favor of our stochastisation hypothesis being the basis for the below analysis of the system in question.

IV. MAPPING

Note that the system in question seems to be similar to one of the Fermi accelerator models, namely, the model of a ball jumping under gravity over an oscillating table [14] (the simplification of Wlam model). Indeed, if we consider the extreme case when the flight time is much larger than the oscillation time (in doing so, the latter tends to zero), then the oscillatory stage of the process can be considered as a shock, and such an analogy is quite suitable. Although some features of these two systems as well as physical mechanisms that control the process are different, the above analogy suggests that the same mathematical description may be used. Thus, the map for the suitable variables is to be defined.

The process time is to be broken down into intervals, each of which contains one flight and oscillations. The beginning of the nth flight is denoted as τ_n, and the beginning of the nth oscillatory stage (the end of the nth flight) is denoted as $\hat{\tau}_n$ (duration of the nth flight is equal to $\Delta\tau_n=\hat{\tau}_n-\tau_n$).

If the initial velocity of bob is V_n, then its displacement during the nth flight is

$$u(\tau_n+\tau)=1+a\sin(\Omega_0\tau_n)+V_n\tau-0.5\tau^2. \quad (7)$$

The flight time, $\Delta\tau_n$, can be defined with the help of the equation

$$1+a\sin(\Omega_0\tau_n)+V_n\Delta\tau_n-0.5\Delta\tau_n^2=1+a\sin[\Omega_0(\tau_n+\Delta\tau_n)]. \quad (8)$$

Note that the right-hand side of Eq. (8) corresponds to the bob position at the end of the flight (the initial bob position for the nth oscillation stage).

The velocity of bob at the end of the nth flight, $\hat{V}_n$ (the initial velocity for nth oscillation stage), is

$$\hat{V}_n=V_n-\Delta\tau_n. \quad (9)$$

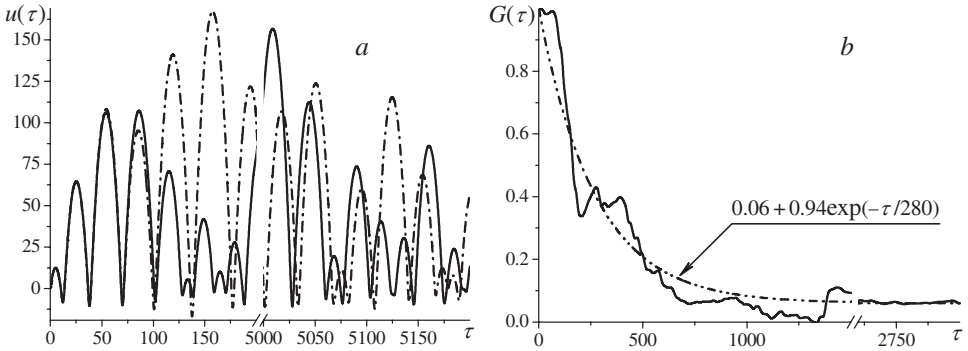

FIG. 4. (a) Two independent numerical solutions of Eqs. (4) and (5) for $a=5$, $\gamma=0.1$, $\Omega_0=1$, and $\delta\tau=0.01$ [the solid line corresponds to solution $u_1(\tau+\delta\tau)$ and the dashed-dotted line to solution $u_2(\tau)$]. (b) Correlation function, $G(\tau)$, for these solutions (the solid line). The dashed-dotted line shows the exponential decay of the correlation function.

The bob displacement during the nth oscillation stage is

$$u(\hat{\tau}_n+\tau)=Ae^{-\gamma\tau}\sin(\sqrt{1-\gamma^2}\tau+\phi)+\frac{a}{\sqrt{(1-\Omega_0^2)^2+(2\gamma\Omega_0)^2}}\sin[\Omega_0(\hat{\tau}_n+\tau)-\varphi], \tag{10}$$

where $\tan\varphi=\frac{2\gamma\Omega_0}{1-\Omega_0^2}$.

The parameters A and ϕ are defined with help of the initial conditions $u(\hat{\tau}_n)=1+a\sin(\Omega_0\hat{\tau}_n)$ and $\dot{u}(\hat{\tau}_n)=\hat{V}_n$,

$$A\sin\phi=1-\frac{a\Omega_0\sqrt{\Omega_0^2+(2\gamma)^2}}{\sqrt{(1-\Omega_0^2)^2+(2\gamma\Omega_0)^2}}\sin(\Omega_0\hat{\tau}_n-\varphi_1), \tag{11}$$

$$A\sqrt{1-\gamma^2}\cos(\phi+\phi_1)=\hat{V}_n-\frac{a\Omega_0}{\sqrt{(1-\Omega_0^2)^2+(2\gamma\Omega_0)^2}}\cos(\Omega_0\hat{\tau}_n-\varphi), \tag{12}$$

where $\tan\varphi_1=\frac{2\gamma/\Omega_0}{1-2\gamma^2-\Omega_0^2}$ and $\tan\phi_1=\frac{\gamma}{\sqrt{1-\gamma^2}}$.

The time of the oscillation stage can be defined with the help of the equation

$$Ae^{-\gamma\Delta\hat{\tau}_n}\sin(\sqrt{1-\gamma^2}\Delta\hat{\tau}_n+\phi)=1-\frac{a\Omega_0\sqrt{\Omega_0^2+(2\gamma)^2}}{\sqrt{(1-\Omega_0^2)^2+(2\gamma\Omega_0)^2}}\sin(\Omega_0\tau_{n+1}-\varphi_1). \tag{13}$$

Finally, we can write the velocity of bob at the end of the nth oscillation stage which is the initial velocity for $(n+1)$th flight,

$$V_{n+1}=Ae^{-\gamma\Delta\hat{\tau}_n}\cos(\sqrt{1-\gamma^2}\Delta\hat{\tau}_n+\phi+\phi_1)+\frac{a\Omega_0}{\sqrt{(1-\Omega_0^2)^2+(2\gamma\Omega_0)^2}}\cos(\Omega_0\tau_{n+1}-\varphi), \tag{14}$$

where

$$\tau_{n+1}=\hat{\tau}_n+\Delta\hat{\tau}_n=\tau_n+\Delta\tau_n+\Delta\hat{\tau}_n. \tag{15}$$

Equations (14) and (15), together with Eqs. (8), (9), and (11)–(13), define the parameters V_{n+1} and τ_{n+1} that depend on the parameters V_n and τ_n for a given a, Ω_0, and γ.

Up to this point all calculations have been exact. Further progress requires simplifications that are based on the smallness of the parameter γ and on the assumption that the flight height significantly exceeds the oscillation amplitude, i.e., for all n the following strong inequality is true:

$$h_n=\frac{1}{2}V_n^2\gg a. \tag{16}$$

The smallness of the parameter γ allows one to simplify Eqs. (11)–(14) and to get the following expression connecting V_{n+1} and $\hat{V}_n$:

$$\left[V_{n+1}-\frac{a\Omega_0\cos(\Omega_0\tau_{n+1}-\varphi)}{\sqrt{(1-\Omega_0^2)^2+(2\gamma\Omega_0)^2}}\right]^2+\left[1-\frac{a\Omega_0^2\sin(\Omega_0\tau_{n+1}-\varphi_1)}{\sqrt{(1-\Omega_0^2)^2+(2\gamma\Omega_0)^2}}\right]^2=\left\{\left[\hat{V}_n-\frac{a\Omega_0\cos(\Omega_0\hat{\tau}_n-\varphi)}{\sqrt{(1-\Omega_0^2)^2+(2\gamma\Omega_0)^2}}\right]^2+\left[1-\frac{a\Omega_0^2\sin(\Omega_0\tau_{n+1}-\varphi_1)}{\sqrt{(1-\Omega_0^2)^2+(2\gamma\Omega_0)^2}}\right]^2\right\}e^{-\gamma\Delta\hat{\tau}_n}. \tag{17}$$

Equation (8) can be presented in a form of the quadratic equation

$$\Delta\tau_n^2-2V_n\Delta\tau_n+4a\sin(\Omega_0\Delta\tau_n/2)\cos[\Omega_0(\tau_n+\Delta\tau_n/2)]=0, \tag{18}$$

and in the case of inequality (16), the parameter $\Delta\tau_n$ in the arguments of the sine and the cosine of Eq. (18) can be assumed to be $2V_n$. The expansion into a power series of the square root of the solution of the obtained quadratic equation results in the following expression for the flight time, $\Delta\tau_n$:

$$\Delta\tau_n\approx 2V_n\left[1-\frac{a}{V_n^2}\sin(\Omega_0V_n)\cos(\Omega_0\tau_n+\Omega_0V_n)\right], \tag{19}$$

and the velocity of bob at the end of the nth flight, $\hat{V}_n$, is

$$\hat{V}_n\approx-\sqrt{V_n^2-2a\sin(\Omega_0V_n)\cos(\Omega_0\tau_n+\Omega_0V_n)}\approx-V_n+\frac{2a}{V_n}\sin(\Omega_0V_n)\cos(\Omega_0\tau_n+\Omega_0V_n). \tag{20}$$

In addition, one can find that the duration of the nth oscillation stage, $\Delta\hat{\tau}_n$, is about

$$\Delta\hat{\tau}_n\approx\pi+\frac{2}{V_n}. \tag{21}$$

Equations (17)–(21) define the required map. However this one is too complicated for the analysis and the further simplifications are necessary.

V. ONE-DIMENSIONAL STOCHASTIC MAP

The obtained two-dimensional map can be reduced to the one-dimensional one. The decrease in the map dimension is possible because of the system's stochastic behavior observed in the numerical solutions (see Figs. 3 and 4). Due to this fact the time moments $\{\hat{\tau}_n\}$ (or $\{\tau_n\}$) can be assumed to be random numbers, i.e., the phases of the arguments of the sines and the cosines in Eq. (17) are random, and the values of this function are also random numbers belonging to the interval $(-1,1)$. In the zero approximation the correlations between the above random variables can be neglected, so that the following conditions take place:

$$\langle\sin(\Omega_0\hat{\tau}_n+\varphi_n)\cdot\cos(\Omega_0\hat{\tau}_m+\psi_m)\rangle_{\{\hat{\tau}\}}=\frac{1}{2}\delta_{n,m},$$

$$\langle \sin(\Omega_0 \hat{\tau}_n + \varphi_n) \cdot \sin(\Omega_0 \hat{\tau}_m + \psi_m) \rangle_{\{\hat{\tau}\}} = 0, \quad \text{for all } n \text{ and } m, \tag{22}$$

where $\langle \ldots \rangle_{\{\hat{\tau}\}}$ denotes the averaging over all $\{\hat{\tau}\}: \langle \cdots \rangle_{\{\hat{\tau}\}} = \Pi_n \Sigma (\frac{\Omega_0}{2\pi} \int \cdots d\hat{\tau}_n)$.

A. Stochastic evolution equation

Based on the above approximation Eq. (17) can be transformed into the following stochastic recursive equation determining the one-dimensional stochastic map:

$$V_{n+1}^2 \approx \exp(-\gamma \Delta \hat{\tau}_n) V_n^2 + \frac{4 V_n a \Omega_0}{\sqrt{(1-\Omega_0^2)^2 + (2\gamma\Omega_0)^2}} \times \left[\sin\left(\frac{\Omega_0 \Delta \hat{\tau}_n}{2}\right) + \frac{\Omega_0}{V_n} \cos\left(\frac{\Omega_0 \Delta \hat{\tau}_n}{2}\right) \right] \times \sin\left(\Omega_0 \frac{2\hat{\tau}_n + \Delta \hat{\tau}_n}{2}\right). \tag{23}$$

The obtained recursive Eq. (23) can be rewritten as a difference equation, and the continuous limit of the latter results in the following stochastic differential equation:

$$\frac{dV(n)}{dn} \approx -\frac{\gamma\pi}{2} V + \theta(V) \sqrt{1 + (\Omega_0/V)^2}\, \xi, \tag{24}$$

where $\theta(V)$ is the step function [$\theta(V)=1$, if $V>0$, and $\theta(V)=0$, if $V \le 0$], and ξ is the stochastic variable with the following characteristics:

$$\overline{\xi} = 0 \quad \text{and} \quad \overline{\xi^2} = \frac{2a^2\Omega_0^2}{(1-\Omega_0^2)^2 + (2\gamma\Omega_0)^2} \sin^2\left(\frac{\pi\Omega_0}{2} + \frac{2\Omega_0}{\bar{V}}\right). \tag{25}$$

B. Fokker-Plank equation

The obtained stochastic Eq. (25) is a nonlinear one, and its solution is not a simple problem. However, the formalism of the Fokker-Plank equation allows one to analyze a linear equation with variable coefficients. It turns out that it is preferable to use the new variable $y = \sqrt{V^2 + \Omega_0^2}$. The stochastic differential equation for this variable is

$$\frac{dy(n)}{dn} = -\frac{\gamma\pi}{2}\left(y - \frac{\Omega_0^2}{y}\right) + \theta(y - \Omega_0)\xi, \tag{26}$$

and the Fokker-Plank equation corresponding to Eq. (26) is

$$\frac{\partial \Phi(y,n)}{\partial n} = \frac{1}{2}\overline{\xi^2} \frac{\partial^2 \Phi(y,n)}{\partial y^2} + \frac{\gamma\pi}{2} \frac{\partial}{\partial y}\left(y - \frac{\Omega_0^2}{y}\right) \Phi(y,n). \tag{27}$$

The boundary conditions for Eq. (27) are

$$\Phi(y = \Omega_0, t) = 0 \quad \text{and} \quad \left.\frac{\partial \Phi}{\partial y}\right|_{y=\Omega_0} = 0. \tag{28}$$

The use of the new variable y results in a noticeable advantage, since the equation describing the second moment of distribution $\Phi(y,n)$ is linear and permits an exact solution. This equation has the following form:

$$\frac{\overline{\partial y^2(n)}}{\partial n} = -\gamma\pi(\overline{y^2(n)} - \Omega_0^2) + \overline{\xi^2}, \tag{29}$$

where $\overline{y^2(t)} = \int y^2 \Phi(y,t) dy$.

VI. HEIGHT OF BOB FLIGHTS

According to the definition of the variable y, one can rewrite Eq. (29) as the equation determining the flight height, $\bar{h} = 0.5\overline{V^2}$, as

$$\frac{\overline{\partial h(n)}}{\partial n} = (-\gamma\pi)\overline{h(n)} + \frac{a^2\Omega_0^2 \sin^2(\pi\Omega_0/2 + 2\Omega_0/\bar{V})}{(1-\Omega_0^2)^2 + (2\gamma\Omega_0)^2}, \tag{30}$$

the exact solution of which, with initial condition $\overline{h(0)} = h_0$, is

$$\overline{h(n)} = \frac{a^2\Omega_0^2 \sin^2(\pi\Omega_0/2 + 2\Omega_0/\bar{V})}{\gamma\pi[(1-\Omega_0^2)^2 + (2\gamma\Omega_0)^2]} + \left\{ h_0 - \frac{a^2\Omega_0^2 \sin^2(\pi\Omega_0/2 + 2\Omega_0/\bar{V})}{\gamma\pi[(1-\Omega_0^2)^2 + (2\gamma\Omega_0)^2]} \right\} e^{-\gamma\pi n}. \tag{31}$$

The desired solution of the problem in question (the averaged height of bob flights) is the stationary solution of Eq. (30), i.e., the asymptotic solution corresponding to large n, which is

$$\bar{h} \simeq \frac{a^2\Omega_0^2}{\gamma\pi[(1-\Omega_0^2)^2 + (2\gamma\Omega_0)^2]} \times \sin^2\left(\frac{\pi\Omega_0}{2} + \frac{\sqrt{\gamma\pi[(1-\Omega_0^2)^2 + (2\gamma\Omega_0)^2]}}{a \sin(\pi\Omega_0/2)}\right). \tag{32}$$

The obtained result has a clear physical interpretation based on the law of energy conservation. Indeed, the elastic energy of the elongated string at the maximum downward displacement is transformed into potential energy of bob. Therefore, the flight height, h, and the amplitude of the forced oscillations, Δ, are related by the following equation:

$$mgh = \kappa\Delta^2/2, \tag{33}$$

which corresponds to the quadratic dependence (32).

The height of bob flights divided by the amplitude of the external force ($\bar{h}/a$) vs dimensionless frequency ($\Omega_0 = \Omega/\omega_0$) is pictured in Fig. 5(a) (solid line). This dependence is of resonant type similar to the resonant dependence of ordinary forced oscillations [see Fig. 5(a), dashed line] and achieves its maximum at the dimensionless frequency $\Omega_0 = 1$, which corresponds to the resonance. Thus, the resonant frequencies in the case of bob flights and in the case of ordinary forced oscillations are the same (within the accuracy of the shift due to damping).

Note that the amplitude of the flights exceeds the amplitude of the forced oscillations by many times. In doing so,

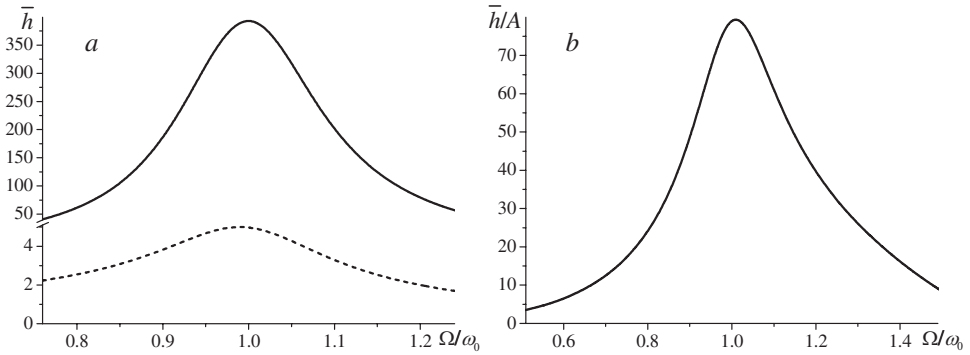

FIG. 5. The resonant curves (a) for the string pendulum which executes the flights (solid line) and for the equivalent spring pendulum which executes ordinary forced oscillations (dash line); (b) for the amplification factor (ratio of the flight height and the amplitude of forced oscillations). The amplitude of the external force, a, and the damping parameter, γ, are the same as the ones used in the numerical calculations ($a=5$ and $\gamma=0.1$).

the amplification factor (ratio of the flight height to the amplitude of forced oscillations) also depends on the frequency of the external force and achieves its maximum at the resonant frequency [see Fig. 5(b)]. For example, in the case of parameter values which were used in the numerical calculations ($a=5$ and $\gamma=0.1$), the amplification factor amounts to about 80. The detected phenomenon of a noticeable increase in the bob displacement in the longitudinal oscillations of a string pendulum is observed also in the numerical calculations, though the latter demonstrates a smaller amplification factor. This fact may be caused by the approximations used during the analytical analysis of the problem in question, e.g., the neglect of the correlation of the oscillation phases for the two successive oscillatory stages, the almost total neglect of damping (except for the case of comparison with the zero members of equations), etc. Nevertheless, the results of the analytical analysis indicate the correct tendency in the features of the examined system.

VII. CONCLUSIONS

The presented analysis of the longitudinal oscillations of a string pendulum has shown that the regime in which the oscillating bob executes free flight under gravity is of great interest from many standpoints. For example, the system in question demonstrates chaotic behavior. A noticeable increase in the bob displacement in the longitudinal oscillations of a string pendulum due to its flights is detected, in doing so, this increase has a resonant character. This phenomenon of the resonant amplitude amplification in the longitudinal oscillations of a string pendulum can find many useful applications.

Finally, let us discuss the mechanism of the resonance phenomenon which was observed in the system in question. It is well known that the physical reason for resonance in the forced oscillations is a synchronization of the moving of the oscillating bob and the oscillations of the external force. The energy pumping into such a system increases when the synchronization improves. On the other hand, for the system executing free flights, the energy pumping is related to the excitation of the free oscillations after each flight. In this case the energy pumping into the system in question is equal to the energy of the excited free oscillations, the amplitude of which is determined by the difference between the bob velocity at the end of the flight and the velocity of the forced oscillations in the corresponding phase. In doing so, in the case of the upward velocity of the forced oscillation the energy pumping increases with the increase in the forced oscillation amplitude and achieves its maximum in resonance, while in the opposite case of the downward velocity of the forced oscillation the energy pumping decreases with the increase in the forced oscillation amplitude. Nevertheless, the average energy pumping through this channel must increase with the amplitude increase in the forced oscillation. It is clear that such a mechanism is most efficient near resonance when the difference between the bob velocity at the end of the flight and the velocity of the forced oscillations decreases. This argument can explain the fact that the resonant height of the bob flights obtained as a result of the numerical solution is lower than that obtained in the analytical calculations, due to accuracy lowering (near resonance) of the approximation used, and perhaps the resonance curve has no pronounced maximum which is to be transformed into a quasiplateau. At the same time, no physical reasons for the shift of the resonant frequency can be formulated. Therefore the resonant frequency of the string pendulum which executes flights can be taken as the fundamental frequency of the string, with a high degree of accuracy. Thus, the mechanism of a resonance phenomenon which is typical only for the string pendulum is described.

ACKNOWLEDGMENTS

The author gratefully acknowledges financial support of the Russell Berrie Nanotechnology Institute, and the United States-Israel Binational Science Foundation under Grant No. 2006061.

[1] *The Pendulum*, edited by M. R. Mattews *et al.* (Springer, New York, 2005).
[2] www.arts.unsw.edu.au/pendulum
[3] Z. J. Jing and J. P. Yang, Int. J. Bifurcation Chaos Appl. Sci. Eng. **16**, 2887 (2006).
[4] J. Awrejcewicz and M. Holicke, Nonlinear Dyn. **47**, 3 (2006).
[5] J. Awrejcewicz, B. Supel, C.-H. Lamarque, G. Kudra, G. Wasilewski, and P. Olejnik, Int. J. Bifurcation Chaos Appl. Sci. Eng. **18**, 2883 (2008).
[6] H. Jo and H. Yabuno, Nonlinear Dyn. **55**, 67 (2009).
[7] J. Miles, J. Acoust. Soc. Am. **75**, 1505 (1984).
[8] A. Kuhn, W. Steiner, J. Zemann, D. Dinevski, and H. Troger, Appl. Math. Comput. **67**, 227 (1995).
[9] A. Goriely, Ph. Boulanger, and J. Leroy, Am. J. Phys. **74**, 784 (2006).
[10] J. Piotrowski, C. R. Mec. **332**, 59 (2004).
[11] D. D. Odhekar, P. S. Gandhiy, and K. B. Joshi, 2005 AIAA Atmospheric Flight Mechanics Conference and Exhibit Online Proceedings, AIAA, San Francisco, 2006).
[12] J. M. W. Brownjohn and T. Botfield, Exp. Tech. **33**, 33 (2009).
[13] M. Burman, A. Arinstein, and E. Zussman, Appl. Phys. Lett. **93**, 193118 (2008).
[14] L. D. Pustylnikov, Dokl. Akad. Nauk SSSR **241**, 1035 (1978).